The Kinetic Energy of the Large-Scale Atmospheric Motion in Wavenumber-Frequency Space: I. Northern Hemisphere

S.-K. KAO[1]

National Center for Atmospheric Research,[2] Boulder, Colo.

AND LARRY L. WENDELL[3]

Dept. of Meteorology, University of Utah, Salt Lake City

(Manuscript received 14 August 1969, in revised form 24 November 1969)

ABSTRACT

The wavenumber-frequency spectra of the kinetic energy of the zonal and meridional components of the motion at 100, 200 and 500 mb, at 20, 40, 60 and 80N, show a definite spectral domain of wave activities in the atmosphere. In middle latitudes, the spectral domain is oriented from a region of low wavenumbers and low frequencies to a region of high wavenumbers and negative frequencies designated for waves moving from west to east. In high latitudes, the domain of wave activities is confined to a region of low wavenumbers and low frequencies. In low latitudes, however, there exist two domains, one similar to that in the middle latitude and the other occurring in a narrow band centered near zero frequency in the medium wavenumber range.

The frequency spectra of the kinetic energy of the zonal motion show similar distributions at all levels and seasons, and are approximately proportional to the minus first power of the frequency in low latitudes but are proportional to the minus second power of the frequency in high latitudes. The wavenumber spectra of the zonal motion also show similar distributions at all levels and seasons, and are approximately proportional to the minus third power of the wavenumber in the high wavenumber range. The wavenumber spectra of the meridional motion show an energy peak in the wavenumber range $k=4$–10. Again, in the high wavenumber range, the power spectra of the meridional motion are approximately proportional to the minus third power of the wavenumber.

The mean kinetic energy of the zonal motion shows a maximum near 40N at all levels and seasons, except at 100 mb in the summer where it occurs near 20N. The distribution of the mean kinetic energy of the moving waves indicates a definite shift in the region of wave activities with height; the maximum wave activity occurs near 60N in the troposphere, near 40N at the tropopause level, and near 60N in the stratosphere. In winter, the mean kinetic energy of the meridional motion shows a great deal of energy in high latitudes, caused primarily by the winter instability of the polar vortex in the stratosphere.

1. Introduction

One of the fruitful lines of studying large-scale atmospheric turbulence and transport processes is the analysis of power and cross spectra of the turbulent motion and transports in the atmosphere. The power spectra, which deal primarily with kinetic, potential, and internal energies, are basic to the understanding of the mechanism of turbulence. The cospectra, which concern primarily the transport and conversion of energies, are fundamental in the maintenance of the general circulation in the atmosphere.

Studies of large-scale turbulence in the free atmosphere have mostly been confined to either space or time spectra of the motion. The Eulerian space (longitude) spectra (Benton and Kahn, 1958; Eliasen, 1958; Kao, 1954; Saltzman, 1958; Barrett, 1961; Van Mieghem, 1961), the Eulerian time spectra (Van der Hoven, 1957; Chiu, 1960; Shapiro and Ward, 1960), and the Lagrangian time spectra (Kao, 1962, 1965; Kao and Bullock, 1964; Kao and Gain, 1968) of the large-scale motion in the atmosphere have recently been analyzed. These investigations have provided a great deal of information regarding the contributions of large-scale atmospheric motion due either to longitude or time eddies. In the atmosphere, however, motion at a point, which is generally nonstationary, is affected by eddies of various sizes and periods. To gain an insight into the mechanism of large-scale atmospheric turbulence and transports, it is necessary to analyze the power and cross spectra in wavenumber-frequency space. Analysis of eddy motions in such a space is, of course, the most general way of studying atmospheric turbulence.

While large-scale motion in the atmosphere may be expressed in terms of spherical harmonics, computations of this type for a long period generally need a great deal of computer time, which proves to be impractical at present. Furthermore, in view of the fact that the

[1] Permanent affiliation: University of Utah.

[2] The National Center for Atmospheric Research is sponsored by the National Science Foundation.

[3] Present Affiliation: ESSA Air Resources Laboratory, Idaho Falls.

mean motion in the atmosphere and the movement of the large-scale atmospheric systems are primarily parallel to latitude circles, the large-scale atmospheric circulation and transport processes may conveniently be examined in the longitude-time space at various altitudes and latitudes. Applications of this type of analysis to various latitude circles would give just about the same result as from the use of spherical harmonics analysis.

In a recent paper (Kao, 1968), a method for analyzing the longitude-time spectra in frequency-wavenumber space was developed. The primary advantage of this method is that it permits analyses of the transient eddies in terms of their length scale and of the speed and direction of their motion; the longitude and time spectra become special cases of the longitude-time spectrum. The relative importance of the forward and backward moving waves may, therefore, be evaluated. With the application of this method, the longitude-time spectra of large-scale atmospheric motions and the meridional transport of angular momentum, and kinetic, potential, and internal energies, have been computed (Kao *et al.*, 1966). In this paper, the longitude-time spectra at 100-, 200- and 500-mb levels, and at 20, 40, 60 and 80N, for the summer and winter, 1964, are presented and investigated.

2. Analysis and data source

In order to make a spectral analysis of large-scale atmospheric motion and transports in frequency-wavenumber space, we make use of the Fourier transform

$$Q(k, \pm n)=\frac{1}{4\pi^2}\int_0^{2\pi}\int_0^{2\pi} q(\lambda,t)e^{-i(k\lambda\pm nt)}d\lambda dt, \quad (1)$$

where λ, t, k and n are the longitude, time, wavenumber and frequency, respectively; $q(\lambda,t)$ is a real, single-valued function, which is piecewise differentiable in a normalized domain, $0\leq\lambda, t\leq 2\pi$; and Q is the complex coefficient of the Fourier transform. The positive and negative signs in front of n are designated to waves moving toward the west and east, respectively.

For convenience of computations in this study, we express

$$Q(k, \pm n)=Q_r(k, \pm n)+iQ_i(k, \pm n), \quad (2)$$

where

$$Q_r(k, \pm n)=\frac{1}{4\pi^2}\int_0^{2\pi}\int_0^{2\pi} q(\lambda,t)\cos(k\lambda\pm nt)d\lambda dt \quad (3)$$

and

$$Q_i(k, \pm n)=\frac{-1}{4\pi^2}\int_0^{2\pi}\int_0^{2\pi} q(\lambda,t)\sin(k\lambda\pm nt)d\lambda dt \quad (4)$$

are the real and imaginary parts, respectively, of the complex coefficient.

Consider the same conditions for another scalar function $s(\lambda,t)$ with a Fourier coefficient $S(k,n)$. It can be shown (Kao, 1968) that

$$\frac{1}{4\pi^2}\int_0^{2\pi}\int_0^{2\pi} s(\lambda,t)q(\lambda,t)d\lambda dt = \sum_{k=0}^{\infty}\int_0^{\infty}[E_{sq}(k, +n)+E_{sq}(k, -n)]dn, \quad (5)$$

and that

$$\left.\begin{aligned} E_{sq}(0, \pm n)&=S_r(0, \pm n)Q_r(0, \pm n)+S_i(0, \pm n)Q_i(0, \pm n)\\ E_{sq}(k, \pm n)&=2[S_r(k, \pm n)Q_r(k, \pm n)+S_i(k, \pm n)Q_i(k, \pm n)], \quad k\neq 0\end{aligned}\right\}, \quad (6)$$

where $E_{sq}(k,+n)$ and $E_{sq}(k,-n)$ are the longitude-time cross spectra of s and q due to eddies of wavenumber k and frequency n, moving toward the west and east, respectively. Eq. (5) indicates that the total contribution of the product of s and q is equal to the cross spectrum of s and q integrated over all frequencies and over all wavenumbers. In (5) the summation of the product of complex coefficient S and Q with respect to the integer wavenumbers is the consequence of the cyclic distribution of $s(\lambda,t)$ and $q(\lambda,t)$ along latitude circles.

The cross spectrum of s and q, due to the eddies of wavenumber k and all frequencies, moving, respectively, toward the west and east is, therefore,

$$E_{sq}(k, \pm)=\int_0^{\infty} E_{sq}(k, \pm n)dn, \quad (7)$$

and the cross spectrum due to eddies of frequency n and all wavenumbers, moving, respectively, in the direction of decreasing and increasing longitude, is

$$E_{sq}(\pm n)=\sum_{k=0}^{\infty} E_{sq}(k, \pm n). \quad (8)$$

Therefore, the longitude and time spectra are, respectively,

$$\left.\begin{aligned} E_{sq}(k)&=\int_0^{\infty}[E_{sq}(k, +n)+E_{sq}(k, -n)]dn\\ E_{sq}(n)&=\sum_{k=0}^{\infty}[E_{sq}(k, +n)+E_{sq}(k, -n)]\end{aligned}\right\}. \quad (9)$$

The horizontal velocities used in this analysis were derived from the 1964 National Meteorological Center (NMC) stream function analyses at the 500- and 200-mb levels, and from the isobaric height field at the 100-mb level. The stream function, isobaric height and temperature distributions were available at 12-hr intervals

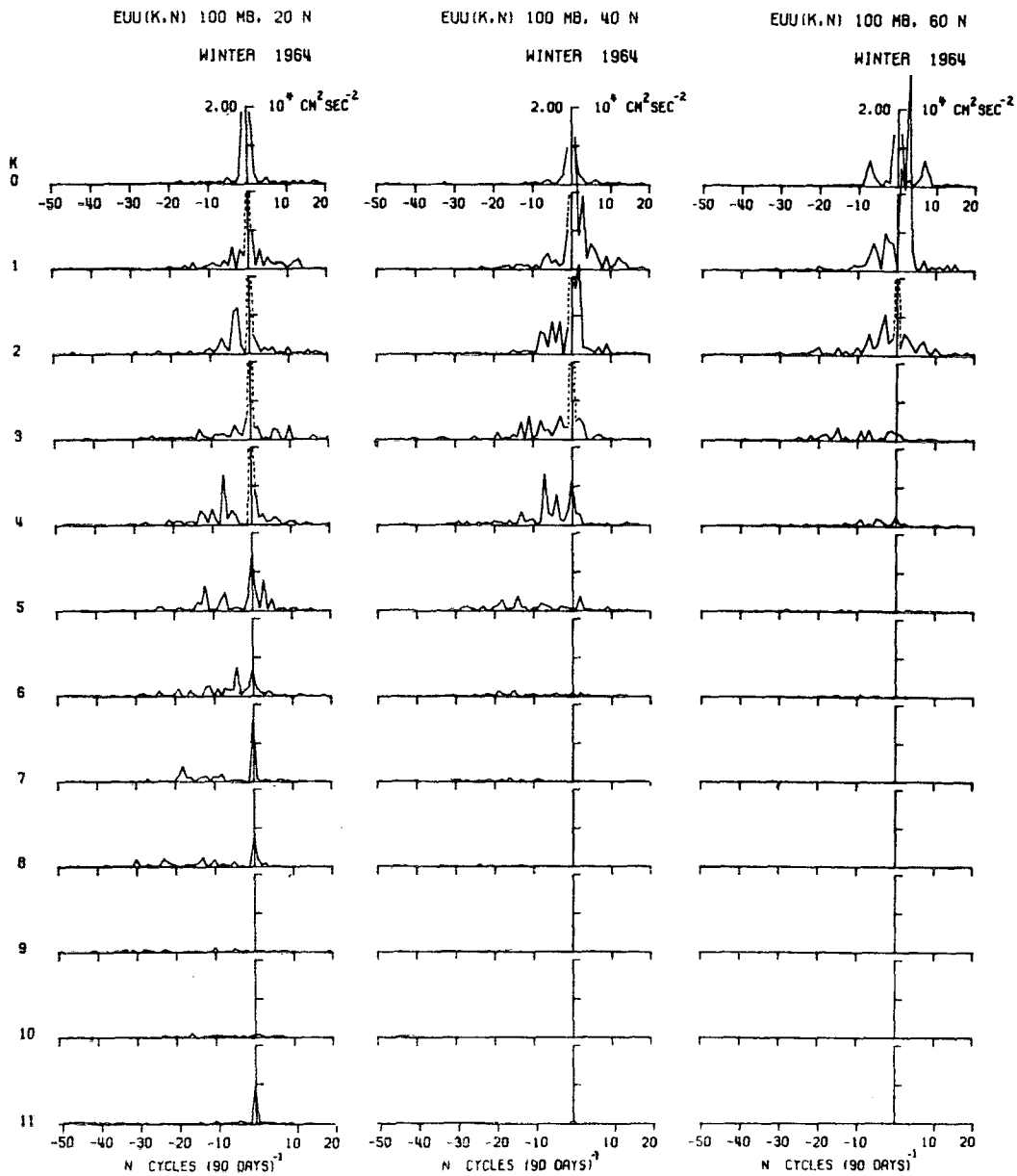

FIG. 1. Wavenumber-frequency spectra of the zonal velocity at 100 mb, winter 1964.

except at the 100-mb level for the summer where a 24-hr interval was used. These functions were interpolated from the grid devised by the Joint Numerical Weather Prediction Unit (JNWP) onto the latitude circles of 20, 40, 60 and 80N, at intervals of 5° of longitude.

The basic computation is the numerical calculation of the real and imaginary parts of Fourier coefficients for various variables. This involves the numerical evaluation of the integrals of (3) and (4) for s, $q=u$, and v. The data intervals used in the integration are 5° of longitude and 12 hr except at 100 mb where 24 hr was used for the summer season. The time integrations were carried out over periods of 90 days for the winter and summer seasons of 1964, which are normalized to 2π. Computations of Fourier coefficients were carried out for a wavenumber range of 0 through 21, and for a frequency range of 0 through 90 cycles per 90 days. The power and co-spectra were computed with the application of Eq. (6) and with the use of the computed Fourier coefficients. However, only the power spectra are analyzed in this paper.

3. The wavenumber-frequency spectra of the zonal and meridional components of the velocity

The mean kinetic energy of the eddy and mean motion in the Northern Hemisphere has been computed and

presented in an earlier paper (Kao and Taylor, 1964). It is found that there exists a region of maximum eddy kinetic energy located to the northwest and slightly below each region of maximum kinetic energy of the mean flow, and that a region of secondary maximum occurs near the surface directly below the primary maximum. Investigations of the distribution and variation of the kinetic energies in relation to the general circulation of the atmosphere indicate that the primary maximum eddy kinetic energy is the result of the convergence of the meridional transport of eddy kinetic energy and the production of the eddy kinetic energy near the jet stream core. The secondary maximum of the eddy kinetic energy is primarily associated with the frontal activities in the lower atmosphere.

In order to investigate the effect of waves of various wavelengths and frequencies on the distribution of the kinetic energy of the large-scale motion in the atmosphere, it is necessary to analyze the longitude-time spectra of the motion in the atmosphere. To do so the wavenumber-frequency spectra of the zonal and meridional components of the velocities at 20, 40, 60 and 80N, at 100-, 200- and 500-mb levels for the summer and winter seasons of 1964, have been computed with the use of Eqs. (3), (4) and (6). Because of the similarity in the spectral distribution for the summer and winter,

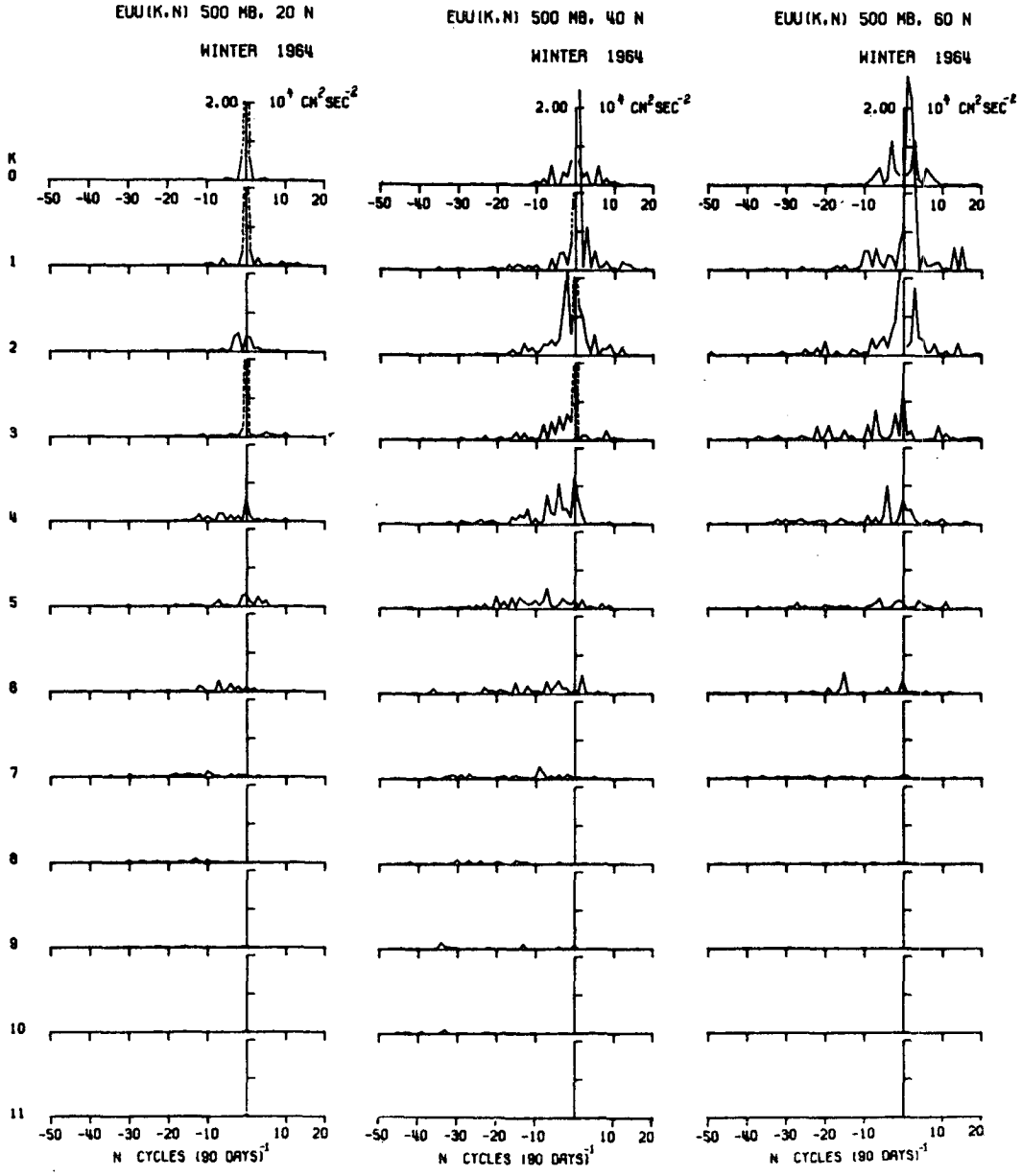

FIG. 2. Wavenumber-frequency spectra of the zonal velocity at 500 mb, winter 1964.

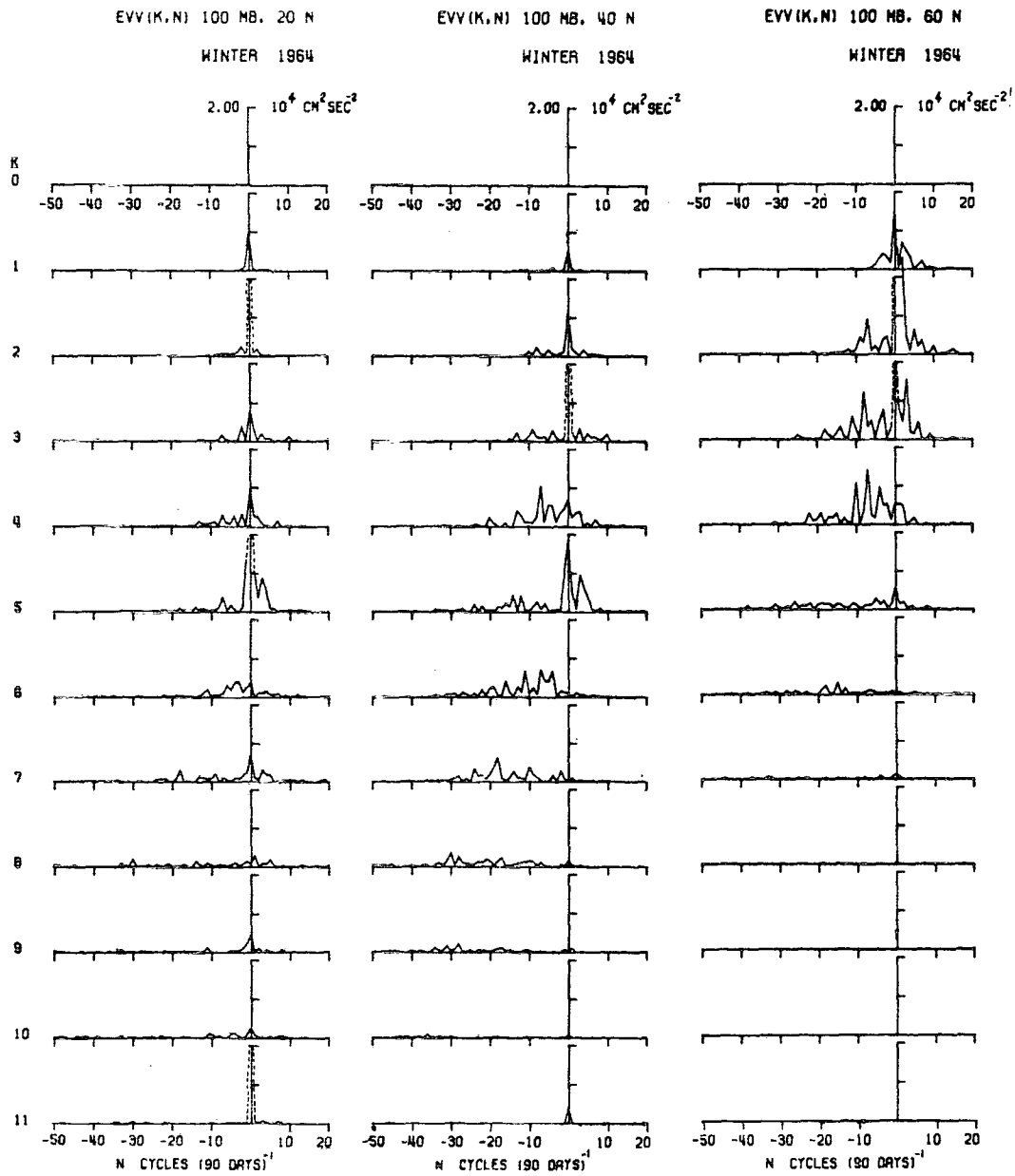

FIG. 3. Wavenumber-frequency spectra of the meridional velocity at 100 mb, winter 1964.

only the power spectra of the velocities at 100- and 500-mb levels at 20, 40 and 60N for the winter season are presented in Figs. 1–4. The magnitude of the spectra for the summer is about half that for the winter. In these figures, the vertical axis represents the spectral eddy kinetic energy, and the horizontal axis the frequency in unit of cycles per 90 days, where positive and negative values designate waves moving from east to west and from west to east, respectively.

It is seen from Figs. 1–4 that there exists a preferred spectral band in the power spectra of the zonal and meridional components of the velocities at various latitudes, which indicates the wavenumber-frequency domain of wave activities. In the middle latitudes (40–60N) the spectral band is oriented in a domain extending from a region of low wavenumbers and frequencies to a region of high wavenumbers and negative frequencies. In the high latitudes (80N), the spectra are confined to a domain of low wavenumbers and frequencies. In low latitudes (20N), however, there exist two domains; in addition to the one similar to that in middle latitudes, a secondary domain occurs in the high wavenumber region confined to a narrow band centered near zero frequency. The change of the orientation of the spectral band with latitude may partially be explained by the increase in the Coriolis effect and

the decrease in the length of the latitudinal circle with increasing latitude on the wave motion in the atmosphere.

It may be noted that wave activities are most pronounced near the tropopause, associating with the maximum mean zonal velocity. The zonal component of the wave is most active in the low and medium wavenumber ranges, whereas the meridional component of the motion is most active in the medium wavenumber range. The intensity of the wave activities in summer is about 50% of that in winter.

It may also be noted that there is a definite shift of the region of wave activities from the troposphere to the stratosphere. In the troposphere, the maximum wave activity occurs in middle latitudes, whereas in the stratosphere, it occurs in low latitudes. This characteristic distribution of the power spectra holds for both the zonal and meridional components of the velocities and for both summer and winter seasons.

To examine further the characteristics of the wavenumber-frequency spectra of the velocity, parallel dashed lines are drawn to form an approximate envelope enclosing the band of significant energy values of the spectra of the meridional velocity at 500 mb, 40N, for winter, as shown in Fig. 4. The frequency envelopes have been plotted as phase-velocity envelopes and are

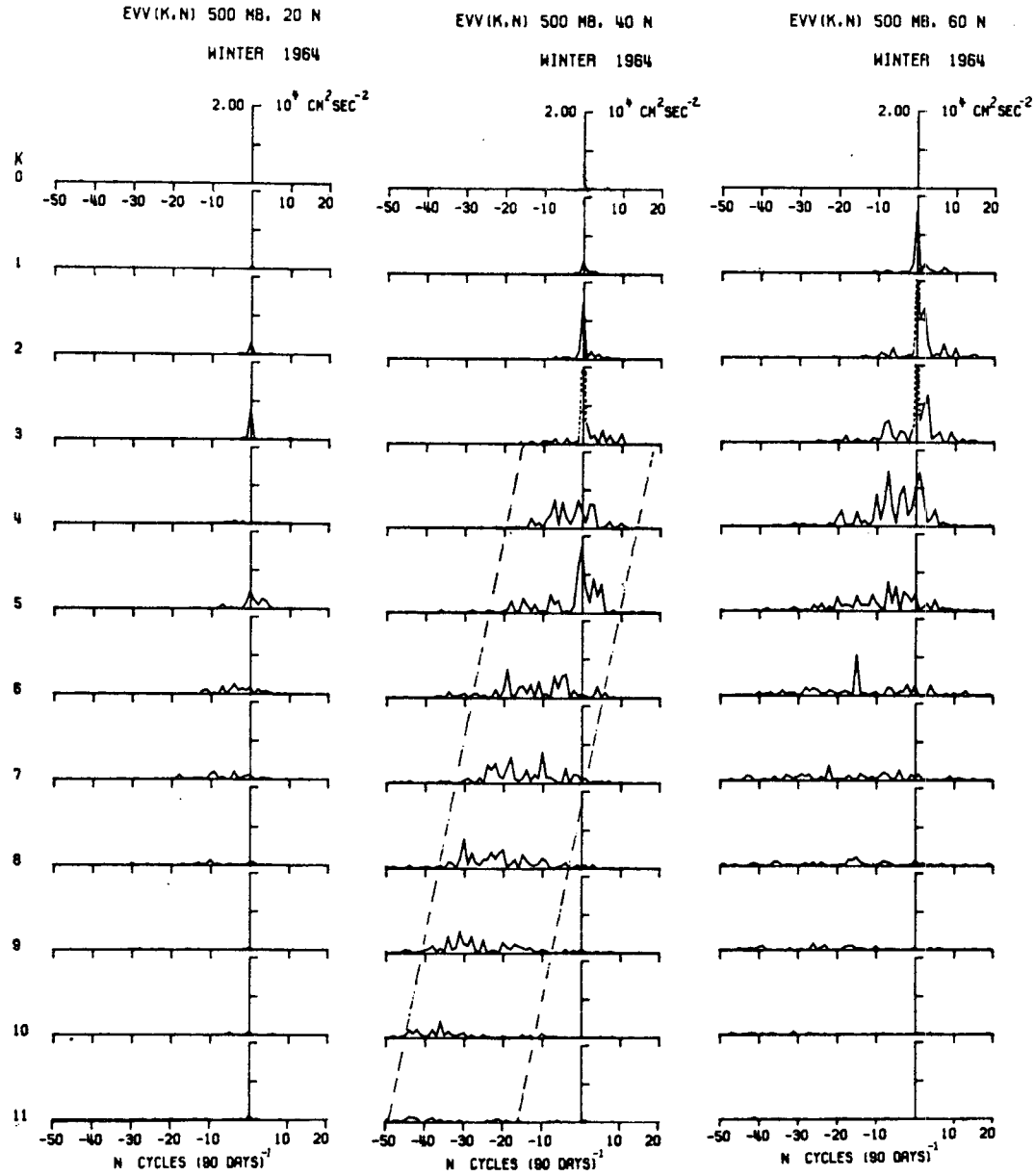

FIG. 4. Wavenumber-frequency spectra of the meridional velocity at 500 mb, winter 1964.

presented by the dashed curves in Fig. 5. For purpose of comparison with the planetary waves in the atmosphere, we consider the particular expression for the phase velocity of long planetary waves (Haurwitz, 1940):

$$C=U-\frac{(\beta L^2/4\pi^2)}{(1+L^2/d^2)}, \tag{10}$$

where U is the mean zonal velocity, L the wavelength, β the latitudinal variation of the Coriolis parameter, and d a measure of the latitudinal extent of the wave. The solid curve in Fig. 5 represents the phase speed computed with the use of (10) for $U=18.5$ m sec^{-1} and $d=10^4$ km. Fig. 5 indicates that wave motion in the atmosphere is essentially of the Rossby type (Rossby, 1939) in which β, U and L are the main parameters.

To make a more complete analysis of the energy spectra of atmospheric motion, it is necessary to examine the contribution of the nonlinear interactions to the energy spectra. To do so, we consider the kinetic energy equations for the zonal and meridional motion, i.e.,

$$\underset{}{\frac{1}{2}\frac{\partial u^2}{\partial t}} = \underset{(u1)}{-\frac{u^2}{a\cos\phi}\frac{\partial u}{\partial\lambda}} \underset{(u2)}{-\frac{uv}{a}\frac{\partial u}{\partial\phi}} \underset{(u3)}{+\frac{\tan\phi}{a}u^2v} + \underset{(u4)}{fu(v-v_g)} + \underset{(u5)}{uF_1}, \tag{11}$$

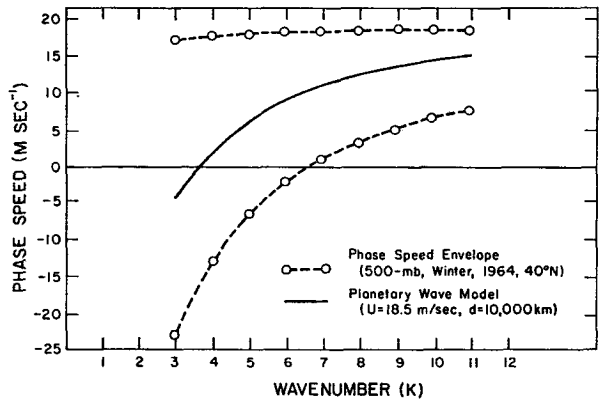

FIG. 5. Comparison of the observed phase speed with the planetary wave model.

$$\underset{}{\frac{1}{2}\frac{\partial v^2}{\partial t}} = \underset{(v1)}{-\frac{uv}{a\cos\phi}\frac{\partial v}{\partial\lambda}} \underset{(v2)}{-\frac{v^2}{a}\frac{\partial v}{\partial\phi}} \underset{(v3)}{-\frac{\tan\phi}{a}u^2v} \underset{(v4)}{-fv(u-u_g)} \underset{(v5)}{+uF_2}, \tag{12}$$

where u_g and v_g are the zonal and meridional components of the geostrophic wind. The numbers below the terms in the equations are for future reference.

The corresponding equations in wavenumber-frequency space for a given value of k and n can be shown to be

$$|U(k,n)|^2=\frac{T}{2\pi}\Big\{U(-k,-n)\underset{(EUU)}{\frac{i}{n}\sum_j\sum_m}\underset{(U1)}{\left[\frac{i}{a\cos\phi}jU(j,m)U(k-j,n-m)\right]}$$
$$+U(-k,-n)\underset{(U2)}{\frac{i}{na}\sum_j\sum_m[U_\phi(j,m)V(k-j,n-m)]}-U(-k,-n)\underset{(U3)}{i\frac{\tan\phi}{na}\sum_j\sum_m[U(j,m)V(k-j,n-m)]}$$
$$-U(-k,-n)\underset{(U4)}{\frac{i}{n}f[V(k,n)-V_g(k,n)]}-\underset{(U5)}{\frac{i}{n}U(-k,-n)G_1(k,n)}\Big\}, \tag{13}$$

$$|V(k,n)|^2=\frac{T}{2\pi}\Big\{V(-k,-n)\underset{(EVV)}{\frac{i}{n}\sum_j\sum_m}\underset{(V1)}{\frac{i}{a\cos\phi}[jV(j,m)U(k-j,n-m)]}$$
$$+V(-k,-n)\underset{(V2)}{\frac{i}{na}\sum_j\sum_m[V_\phi(j,m)V(k-j,n-m)]}+V(-k,-n)\underset{(V3)}{\frac{i\tan\phi}{na}\sum_j\sum_m[U(j,m)U(k-j,n-m)]}$$
$$+V(-k,-n)\underset{(V4)}{\frac{i}{n}f[U(k,n)-U_g(k,n)]}-\underset{(V5)}{\frac{i}{n}V(-k,-n)G_2(k,n)}\Big\}, \tag{14}$$

where $U_g(k,n)$ and $V_g(k,n)$ are the transforms of the zonal and meridional components of the geostrophic wind. Again the symbols below the terms on the right side of the equations are for future reference. The summations over the index j are from $-j_s$ to $+j_s$, where j_s depends on the number of discrete points on the latitude circle. The summations over m are from $\mp m_s$ to $\pm m_s$ depending on whether frequency n is positive or negative, where m_s depends on the number of discrete time data points used.

TABLE 1. Linear and nonlinear contributions to the kinetic energy of the zonal motion in various wavenumber-frequency domains.*

	$EUU=$	$U1$	$+$ $U2$	$+$ $U3$	$+$ $U4$	$+$ $(U5+E_1)$
$(P,-L)$	16.83=	75.81	−13.06	−0.13	−49.16	+3.37
$(P,+L)$	13.39=	−59.85	+15.79	+1.09	+44.94	+11.42
$(P,-I)$	7.12=	8.39	+1.55	+0.08	−3.65	−0.75
$(C,-L)$	2.64=	18.37	−10.26	−1.03	−2.20	−2.24
$(C,+L)$	1.12=	−11.15	+7.60	+0.28	+0.79	+3.50
$(C,-I)$	3.35=	6.74	−1.04	−0.08	−2.27	+0.00

* E_1 is the data error.

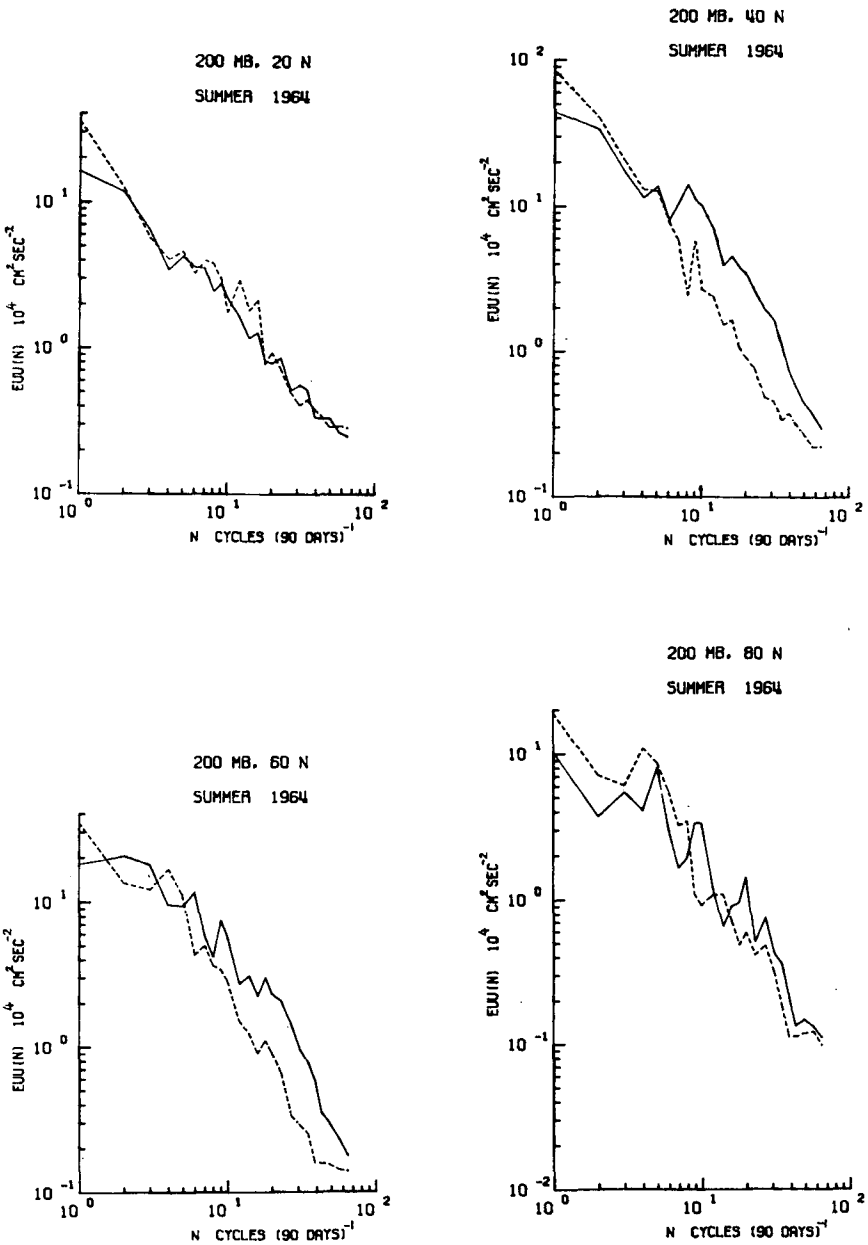

FIG. 6. Frequency spectra of the zonal velocity at 200 mb, summer 1964. The solid and dashed curves represent the spectra contributed by the waves moving from west to east and from east to west, respectively.

TABLE 2. Linear and nonlinear contributions to the kinetic energy of the meridional motion in various wavenumber-frequency domains.*

	$EVV=$	$V1$	$+ V2$	$+ V3$	$+ V4+(V5+E_2)$
$(P, -L)$	7.31=	48.67	−15.28	+4.33	−48.72 +18.31
$(P, +L)$	7.85=	−49.92	+11.61	+1.11	+51.80 −6.75
$(P, -I)$	2.56=	5.31	+0.29	+0.31	−4.01 +0.66
$(C, -L)$	5.80=	32.19	−0.28	−2.47	−23.83 +0.19
$(C, +L)$	1.52=	−13.21	+2.48	+0.07	+7.97 +4.21
$(C, -I)$	15.11=	30.40	−1.63	−0.29	−12.17 −1.20

* E_2 is the truncation error.

It is found that the nonlinear interactions in wavenumber-frequency space contribute primarily to the spectral kinetic energy in the domain of low-frequency eastward and westward moving planetary waves, the intermediate-frequency eastward moving planetary waves, the low-frequency eastward and westward moving cyclone waves, and the intermediate-frequency eastward moving cyclone waves, denoted, respectively, by $(P, -L)$, $(P, +L)$, $(P, -I)$, $(C, -L)$, $(C+L)$ and $(C, -I)$. These magnitudes of these contributions both

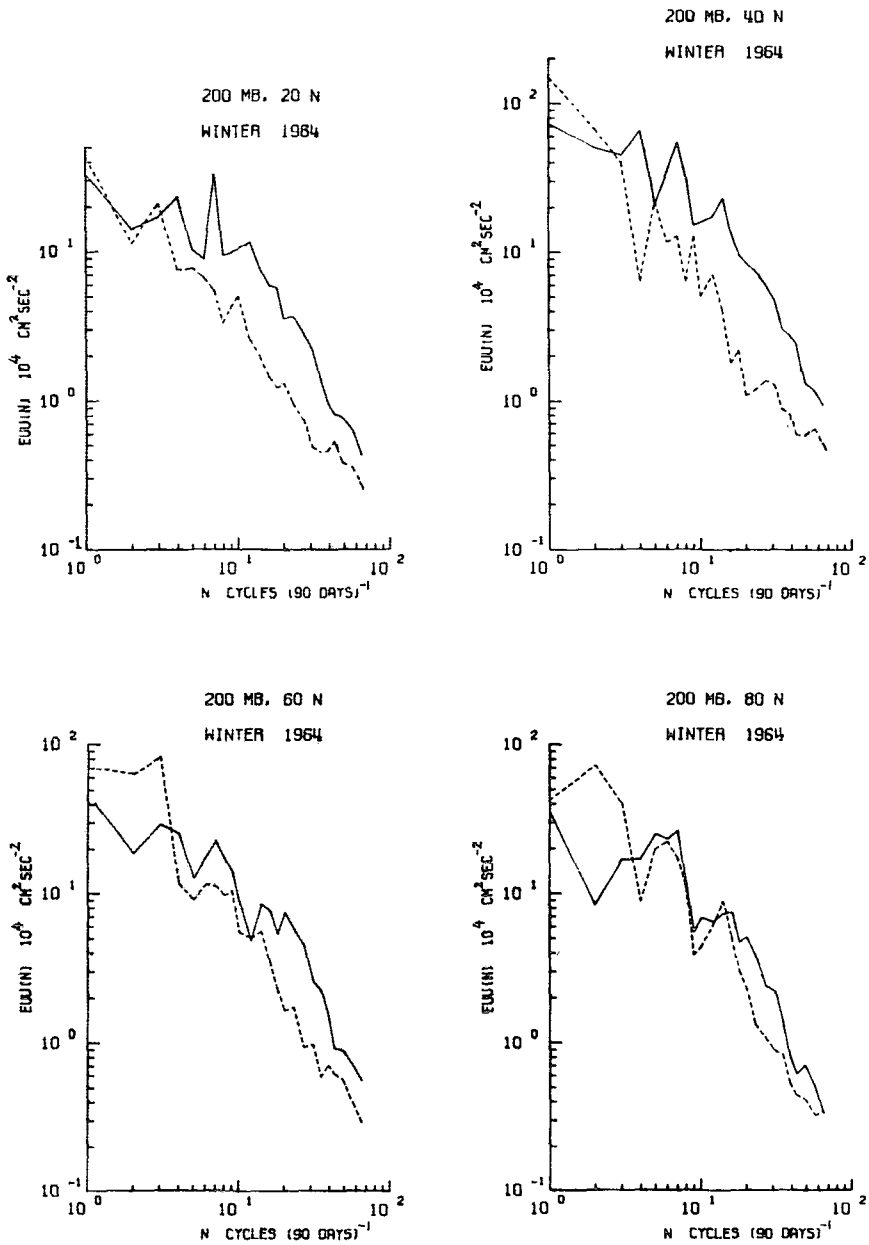

FIG. 7. Frequency spectra of the zonal velocity at 200 mb, winter 1964. The solid and dashed curves have the same representation as in Fig. 6.

to zonal and meridional motions are shown in Tables 1 and 2, respectively, where E_1 and E_2 are the data and the truncation errors.

The following characteristics of the linear and nonlinear contributions to the spectral kinetic energy in various wavenumber-frequency domains may be noted from the above tables:

1) The resultant of the nonlinear interactions due to the longitudinal convergence of the flux of kinetic energy ($U1,V1$) always supplies kinetic energy to the eastward moving waves, but abstracts kinetic energy from the westward moving waves.

2) The nonlinear interactions due to the latitudinal convergence of the flux of kinetic energy ($U2,V2$) are generally smaller than and of the opposite sign to those due to the longitudinal convergence of the flux of kinetic energy ($U1,V1$).

3) The ageostrophic mechanism ($U4,V4$) always supplies kinetic energy to the westward moving waves, but abstracts kinetic energy from the eastward moving waves.

4) The magnitude of the frictional effect ($U5,V5$) generally decreases with decreasing wavelength of the waves.

5) The sphericity effect of the earth ($U3,V3$) is generally small and may be neglected.

It is also found from the analysis of the nonlinear interactions that the main contribution of the inertia

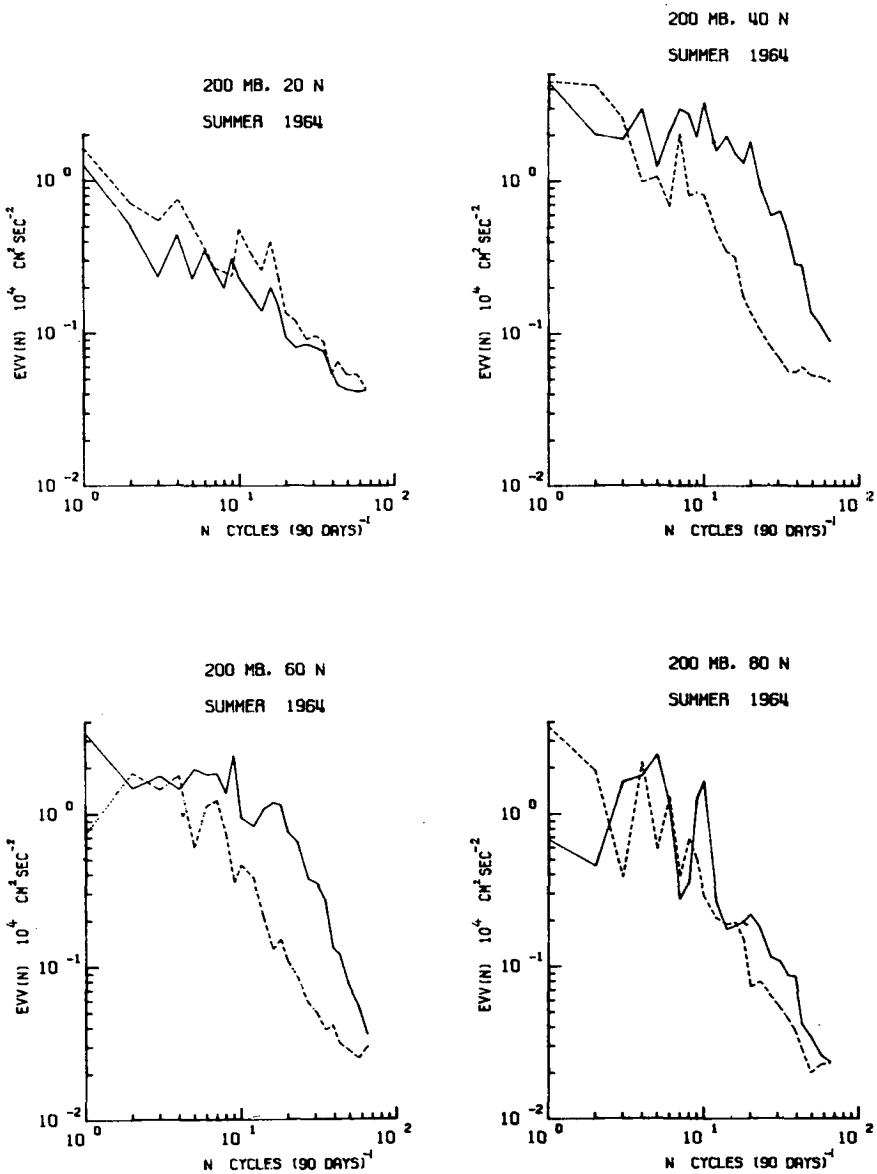

FIG. 8. Frequency spectra of the meridional velocity at 200 mb, summer 1964. The solid and dashed curves have the same representation as in Fig. 6.

interactions always involves the mean zonal motion. The results of an elaborate analysis of the nonlinear interactions in wavenumber-frequency space will be reported in a separate paper (Wendell, 1969).

4. The power spectra of the zonal and meridional components of the velocity in the frequency and wavenumber domains

The distribution of the power spectra of the zonal and meridional components of the velocity in the frequency domain at the 100-, 200- and 500-mb levels and at 20, 40, 60 and 80N for the summer and winter seasons of 1964, have been computed with the use of Eqs. (6) and (8). Because of the similarity in the spectral distribution at the above-mentioned levels, only the spectra at the 200-mb level are shown in Figs. 6–9. In these figures, the solid curves are the frequency spectra of the velocity contributed by waves moving from west to east, and the dashed curves are those contributed by waves moving from east to west.

It is seen from Figs. 6 and 7 that the power spectra of the zonal components of the velocity generally decrease with increasing frequency, and that there are more wave activities in winter than in summer. It may be noted that there is more kinetic energy involved in waves moving from west to east than in waves moving

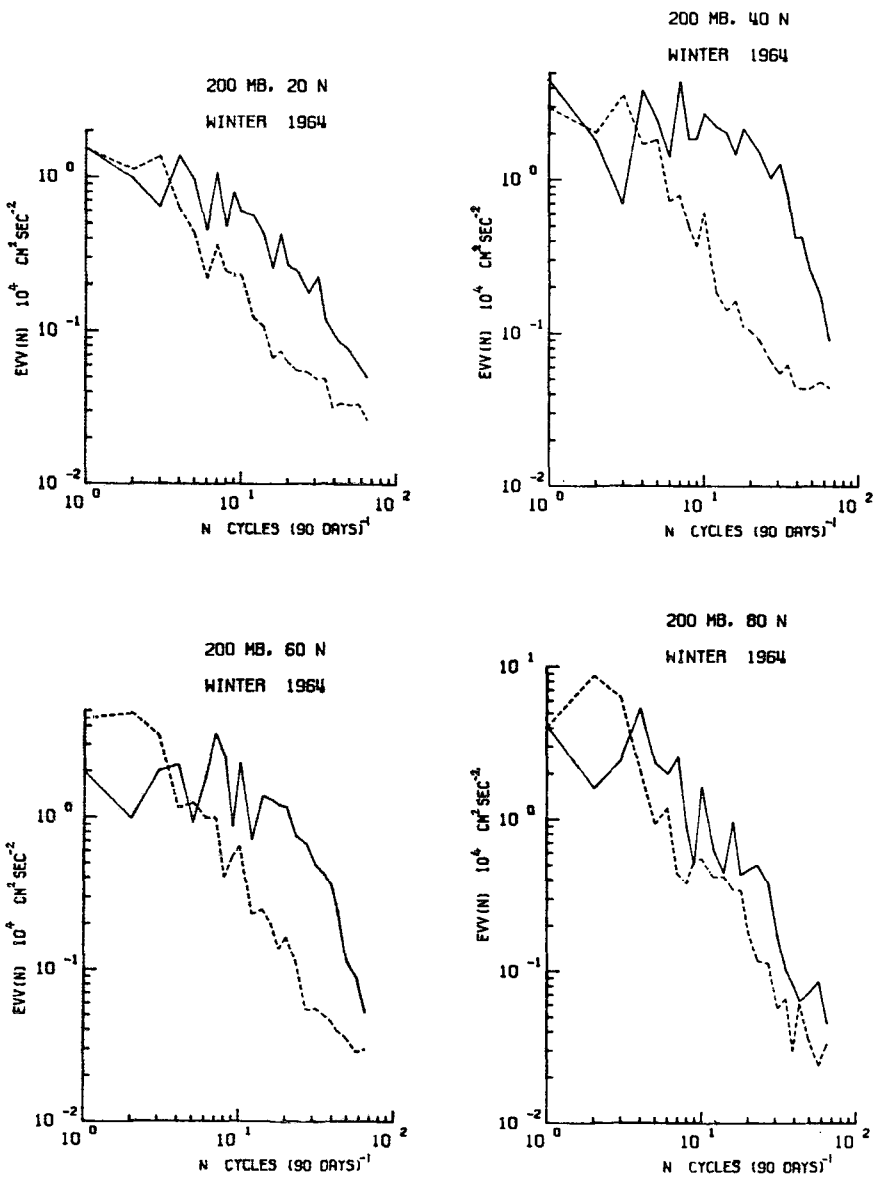

FIG. 9. Frequency spectra of the meridional velocity at 200 mb, winter 1964. The solid and dashed curves have the same representation as in Fig. 6.

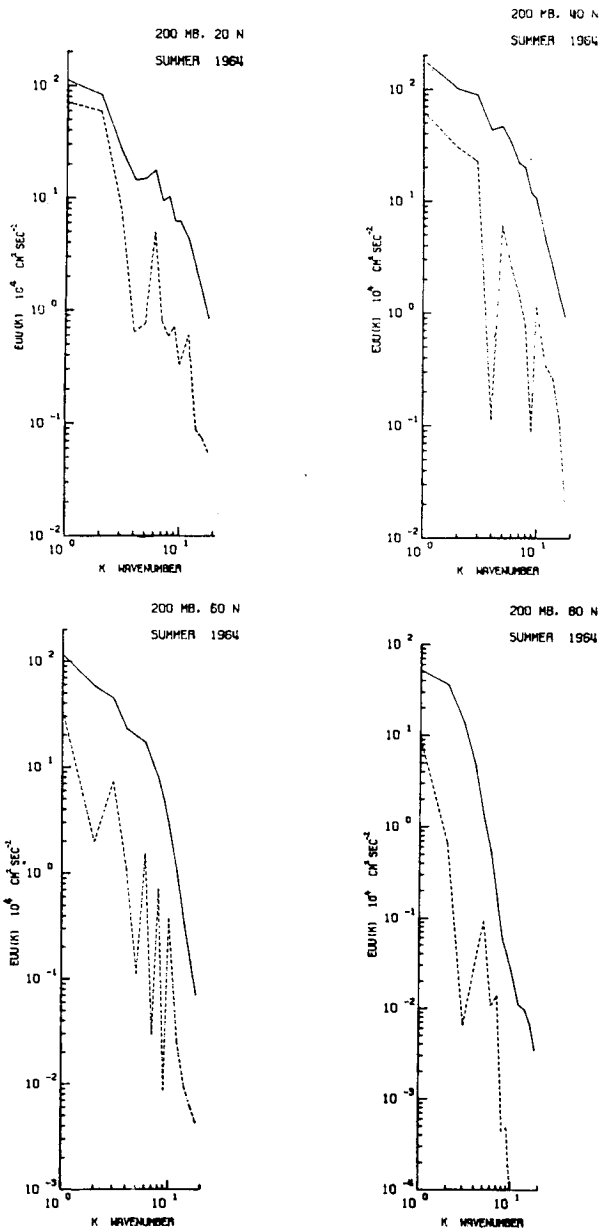

FIG. 10. Wavenumber spectra of the zonal velocity at 200 mb, summer 1964. The solid and dashed curves connecting the points of line spectra represent the contribution made by the total motion and the stationary waves, respectively.

from east to west, except in the low-frequency range of the spectra.

The distribution of the power spectra of the meridional component of the velocity at 200 mb in the frequency domain shown in Figs. 8 and 9 indicates characteristics similar to those of the zonal velocity component. However, the power spectra of the meridional component of waves moving from west to east show energy peaks in the frequency range from 4–20 cycles $(90 \text{ days})^{-1}$.

In the high-frequency range of the spectra, the kinetic energy of the zonal and meridional components of the motion is approximately proportional to the minus first power of the frequency in low latitudes but is proportional to the minus second power of the frequency in high latitudes.

The distributions of the power spectra of zonal and meridional velocities at 200 mb in the wavenumber domain are shown in Figs. 10–13. In these figures, as a

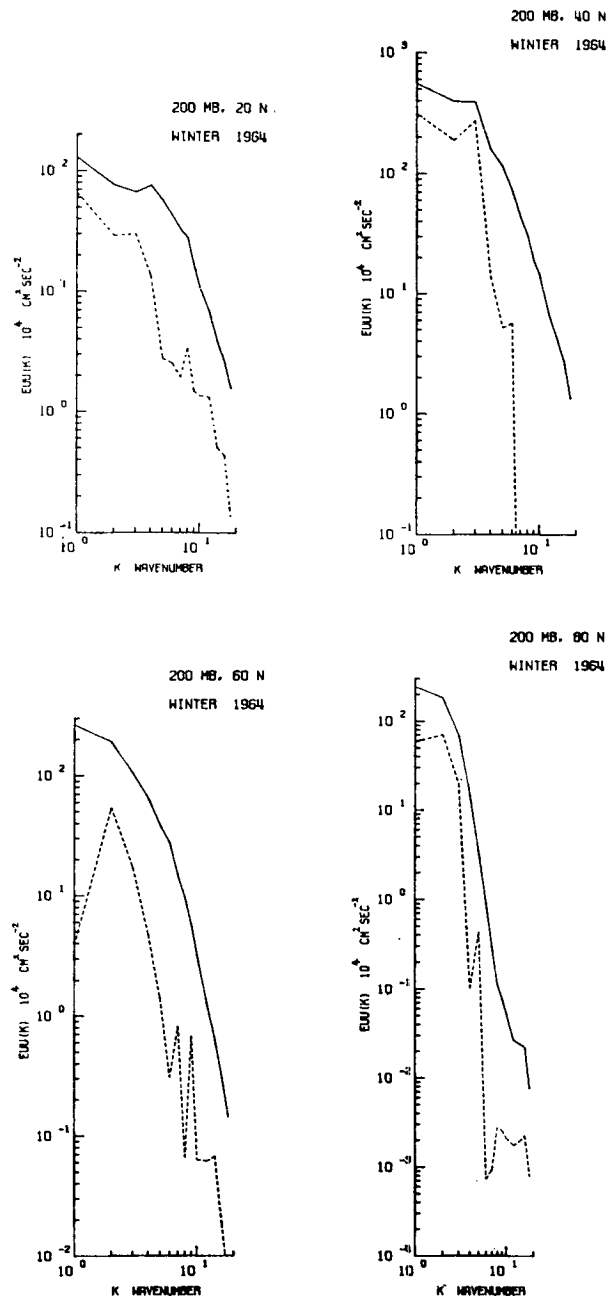

FIG. 11. Wavenumber spectra of the zonal velocity at 200 mb, winter 1964. The solid and dashed curves have the same representation as in Fig. 10.

visual aid, the points of line spectra are connected by solid and dashed lines. The solid lines represent the contribution made by the stationary and nonstationary waves, whereas the dashed curves represent that made by the stationary waves. It is seen from these figures that most of the kinetic energy is contributed by the moving waves, and that the kinetic energy of the motion in winter is greater than that in summer. In the high-wavenumber range, the energy spectra of both the zonal and meridional motion are approximately proportional to the minus third power of the wavenumber.

In their studies of the two-dimensional turbulence of an incompressible, nonrotating viscous fluid, Kraichnan (1967), Leith (1968) and Lilly (1969) have found that the entropy of the motion is transferred to the higher wavenumbers through a k^{-3} spectrum, whereas the energy is transferred to the lower wavenumbers through a $k^{-5/3}$ spectrum. The spectral behavior in the high-wavenumber range is very much similar to those shown in Figs. 10–13. The long atmospheric waves shown in Fig. 5 depend indeed on the latidinal variation of the Coriolis parameter. However, in the high-wavenumber range the effect of β becomes small, and the spectral behavior of the motion in a rotating system is practically similar to that in a nonrotating system.

The wavenumber spectra of the zonal velocity (Figs. 10 and 11) generally decrease with increasing wavenumber, whereas those of the meridional velocity (Figs. 12 and 13) show an energy peak in the wavenumber range $k=4$–10. It may be noted that there is no kinetic energy involved in the power spectra of the meridional velocity at the wavenumber zero, since the zonal mean of the meridional velocity computed from the stream function is zero.

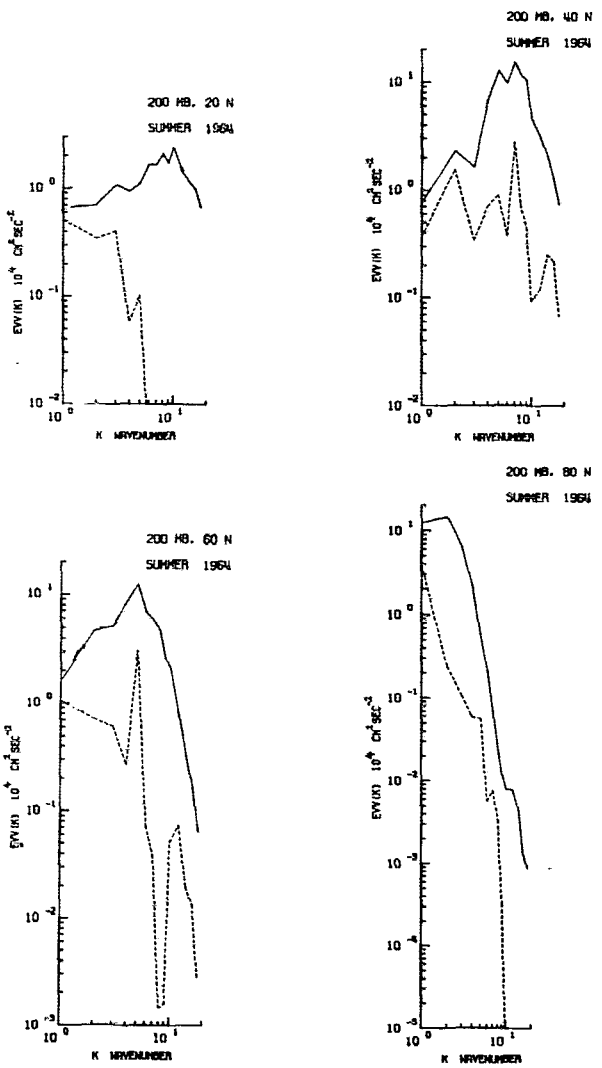

FIG. 12. Wavenumber spectra of the meridional velocity at 200 mb, summer 1964. The solid and dashed curves have the same representation as in Fig. 10.

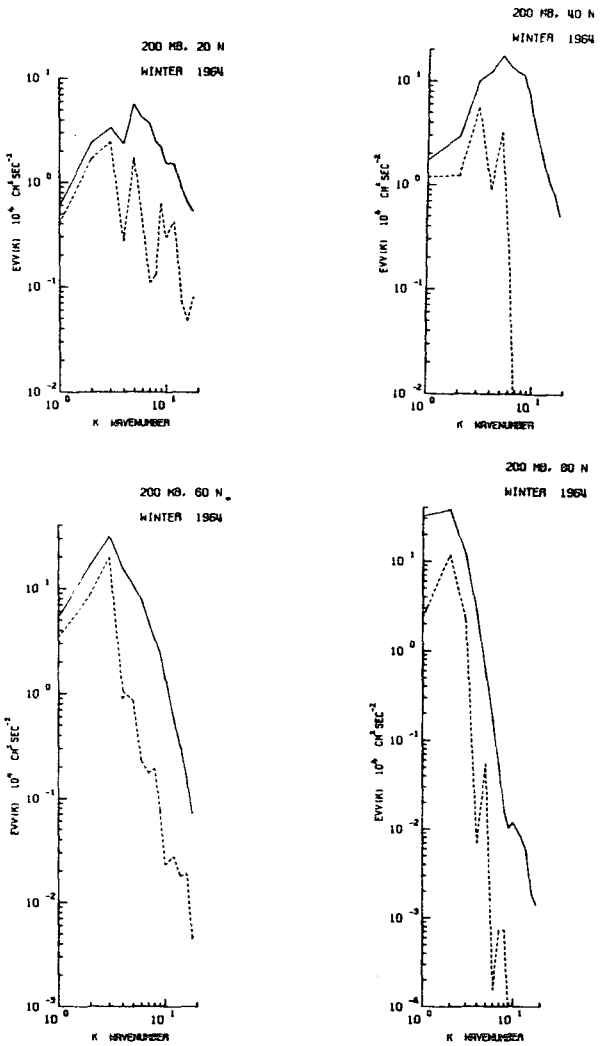

FIG. 13. Wavenumber spectra of the meridional velocity at 200 mb, winter 1964. The solid and dashed curves have the same representation as in Fig. 10.

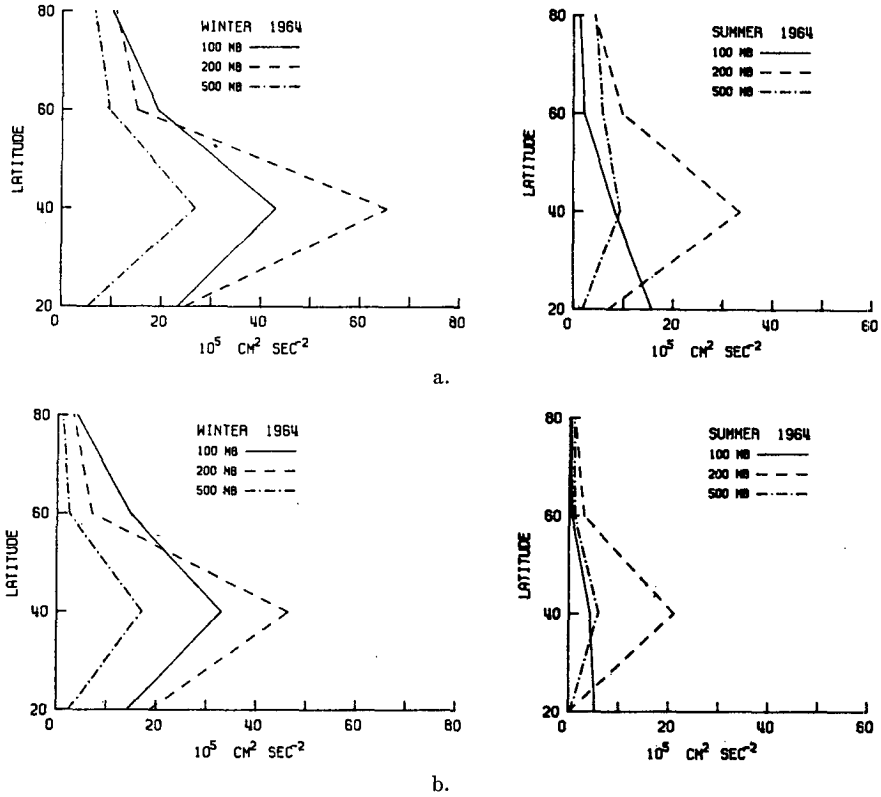

FIG. 14. Mean kinetic energy of the zonal motion, a., and of the zonal component of the stationary zonal mean motion, b.

The distributions of the frequency and wavenumber spectra of the zonal and meridional components of the velocity at the 100- and 500-mb levels are similar to those at the 200-mb level, except that the kinetic energy level at 100 and 500 mb is smaller than at 200 mb.

5. The mean kinetic energy of the zonal and meridional components of the velocity

To examine the characteristics of the distribution of the mean kinetic energy in the atmosphere, it is convenient to express the mean kinetic energy of the ith component of the motion as

$$\sum_k \sum_n E_{ii}(k,n) = E_{ii}(0,0) + \sum_{n\neq 0} E_{ii}(0,n) + \sum_{k\neq 0} E_{ii}(k,0) + \sum_{k\neq 0} \sum_{n\neq 0} E_{ii}(k,n), \quad (15)$$

where $i=u$, v, the first term on the right-hand side of the equation is the kinetic energy of the ith component of the stationary zonal mean motion, the second term that of the nonstationary zonal mean motion, the third that of the stationary wave motion, and the last that of the nonstationary wave motion. The values of these terms for the zonal and meridional components of the motion are plotted in Figs. 14 and 15. It may be noted that for the meridional component of the motion, the first and third terms on the right-hand side of the above equation, are zero, since the zonal mean of the meridional velocity computed from the stream function is zero.

It is seen from Fig. 14a that the mean kinetic energy of the zonal component of the total motion in winter is about twice that in summer, and that the maximum kinetic energy at all levels for both summer and winter occurs near 40N, except that at 100 mb in summer it occurs near 20N.

The distribution of the kinetic energy of the zonal component of the stationary zonal mean motion (Fig. 14b) for both summer and winter seasons is very much similar to that of the total motion, and represents about two-thirds of the kinetic energy of the zonal component of the total motion.

The kinetic energy of the zonal component of the nonstationary zonal mean motion (Fig. 15a) is small as compared with the other terms in Eq. (15). However, its maximum kinetic energy occurs near 80N.

The distribution of the kinetic energy of the zonal component of the stationary wave motion in the winter (Fig. 15b) is similar to that of the zonal component of the total motion. However, in the summer the distribution is quite different; the maximum of the kinetic

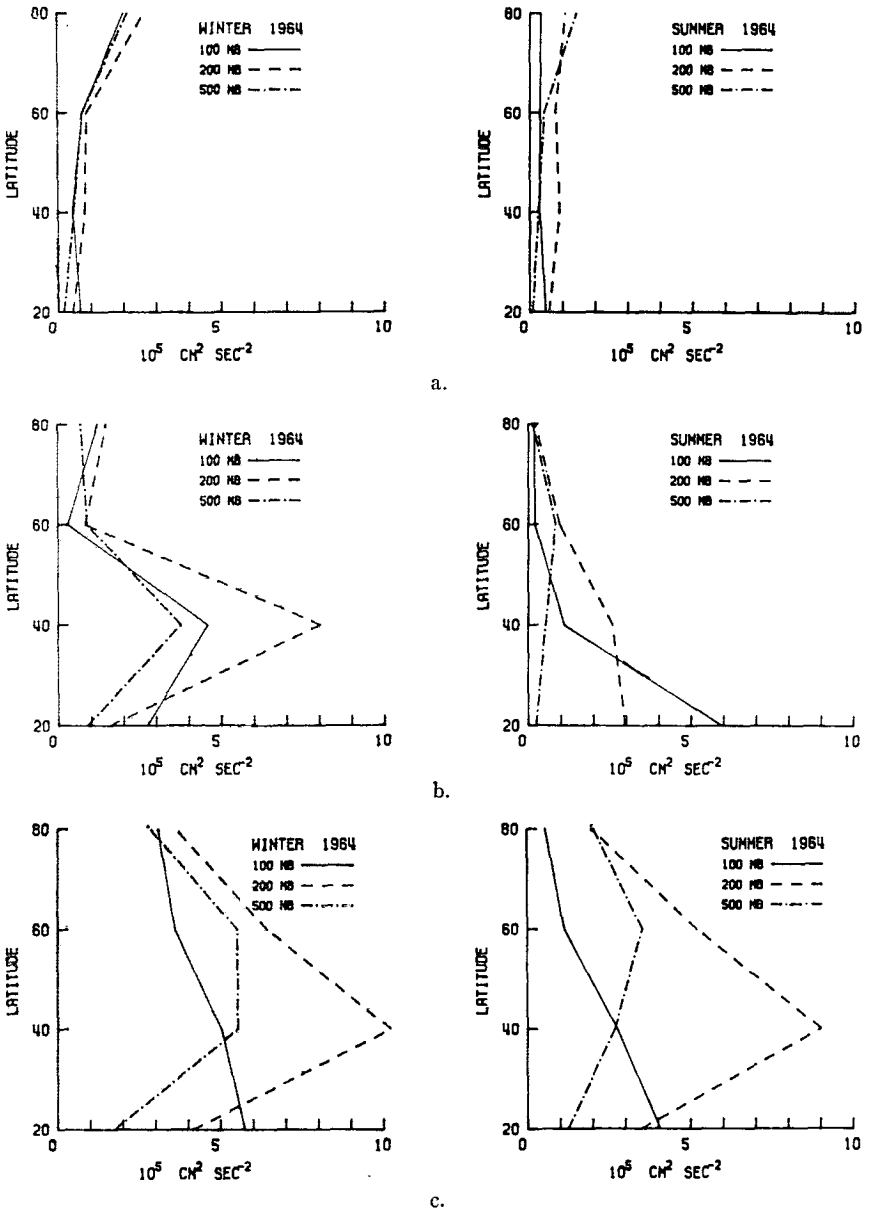

FIG. 15. Mean kinetic energy of the zonal component of the nonstationary zonal mean motion, a., of the zonal component of the stationary waves, b., and of the zonal component of the moving waves, c.

energy in the stratosphere and at the tropopause occurs near 20N.

The distribution of the kinetic energy of the zonal component of the moving waves (Fig. 15c) is rather different from that of the total zonal motion. In the troposphere, the maximum kinetic energy of the moving waves for both the summer and winter seasons occurs near 60N; however, in the stratosphere, it occurs near 40N at 200 mb and near 20N at 100 mb, indicating that the region of activity of moving waves shifts from high latitudes in the troposphere to low latitudes in the stratosphere. It may be noted that moving waves are most active near the jet stream core. However, the kinetic energy of the moving waves maintains about the same level for summer and winter, although in the winter it is slightly greater than that in the summer.

The distribution of the kinetic energy of the meridional component of the total motion in the summer as shown in Fig. 16a is similar to that of the moving waves in the summer (Fig. 16c), since the kinetic energy involved in the stationary wave is very small (Fig. 16b). It may be noted that the kinetic energy of the meridional velocity of the moving waves is very similar to that of the zonal velocity of the moving waves; the maximum

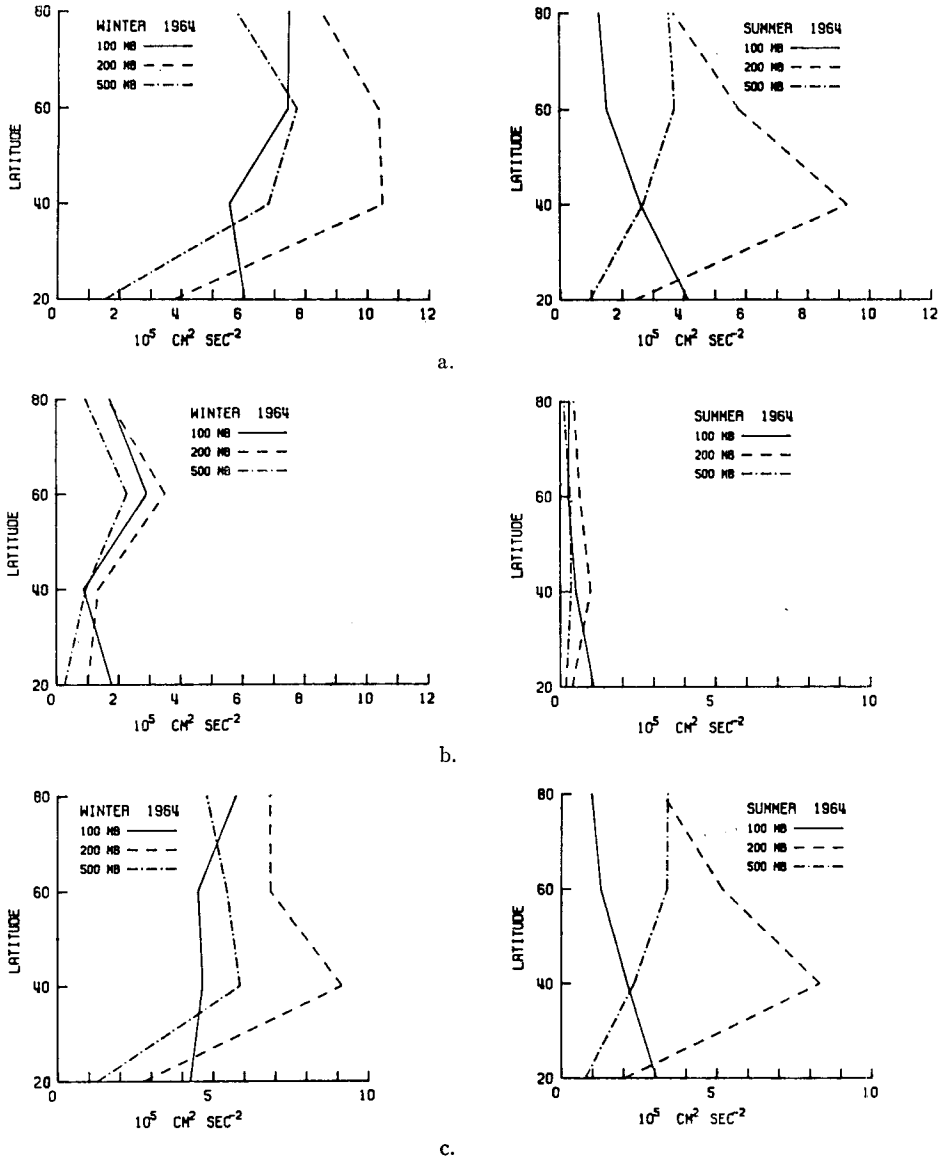

FIG. 16. Mean kinetic energy of the meridional motion, a., of the meridional component of the stationary waves, b., and of the meridional component of the moving waves, c.

of the kinetic energy of both the zonal and meridional velocities occurs near 20N at 100 mb, near 40N at 200 mb, and near 60N at 500 mb.

The distribution of kinetic energy of the meridional component of the motion in winter (Fig. 16a) indicates that the maximum of the kinetic energy of the meridional motion occurs near 60N at 500 mb and near 40N at 200 mb; at 100 mb there are two maxima, the primary one occurring near 80N and the secondary near 20N. The abundant kinetic energy occurring at high latitudes in the winter stratosphere is probably due to the winter instability of the polar vortex in the stratosphere. It may be noted that most of the kinetic energy of the meridional component of the motion is due to the activity of the moving waves, only a small portion of the kinetic energy of the meridional motion being involved in the stationary waves. It may also be noted that moving waves are most active near the jet stream core.

Acknowledgments. This research has been partly supported by the Division of Biology and Medicine of the U. S. Atomic Energy Commission, under Contract AT(11-1)-1585.

REFERENCES

Barrett, E. W., 1961: Some applications of harmonic analysis to the study of general circulation. *Beitr. Phys. Atmos.*, **33**, 280–355.

Benton, G. S., and A. B. Kahn, 1958: Spectra of large-scale atmospheric flow at 300 millibars. *J. Meteor.*, **15**, 404–410.

Chiu, W.-C., 1960: The wind and temperature of the upper troposphere and lower stratosphere over North America. *J. Meteor.*, **17**, 64–77.

Eliasen, E., 1958: A study of the long atmospheric waves on the basis of zonal harmonic analysis. *Tellus*, **10**, 206–215.

Haurwitz, B., 1940: The motion of atmospheric disturbances on the spherical earth. *J. Marine Res.*, **3**, 354–367.

Kao, S.-K., 1954: An analysis of the longitudinal spectrum of the large-scale atmospheric motion. *Bull. Amer. Meteor. Soc.*, **35**, 84; see also AFCRL Tech. Rept. 54 260, Final Rept., Vol. 1, Dept. Civil Engineering, Johns Hopkins Univ., 235–244.

——, 1962: Large-scale turbulent diffusion in a rotating fluid with applications to the atmosphere. *J. Geophys. Res.*, **67**, 2347–2359.

——, 1965: Some aspects of the large-scale turbulence and diffusion in the atmosphere. *Quart. J. Roy. Meteor. Soc.*, **91**, 10–17.

——, 1968: Governing equations and spectra for atmospheric motion and transports in frequency wavenumber space. *J. Atmos. Sci.*, **25**, 32–38.

——, and W. S. Bullock, 1964: Lagrangian and Eulerian correlations and energy spectra of geostrophic velocities. *Quart. J. Roy. Meteor. Soc.*, **90**, 166–174.

——, and A. A. Gain, 1968: Large-scale dispersion of clusters of particles in the atmosphere. *J. Atmos. Sci.*, **25**, 214–221.

——, and V. R. Taylor, 1964: Mean kinetic energies of the eddies and mean currents in the atmosphere. *J. Geophys. Res.*, **69**, 1037–1049.

——, L. L. Wendell and D. A. Noteboom, 1966: Longitude-time power- and cross-spectra of atmospheric quantities. Res. Rept. on Atmospheric Turbulence and Transport, University of Utah, 240 pp.

Kraichnan, R. H., 1967: Inertial ranges in two-dimensional turbulence. *Phys. Fluids*, **10**, 1417–1423.

Leith, C. E., 1968: Diffusion approximation for two-dimensional turbulence. *Phys. Fluids*, **11**, 671–673.

Lilly, D. K., 1969: Numerical simulation of two-dimensional turbulence. *Phys. Fluids*, **12** (in press).

Rossby, C. G., 1939: Relation between variations in the intensity of the zonal circulation of the atmosphere and the displacement of the semipermanent centers of action. *J. Marine Res.*, **2**, 38–55.

Saltzman, B., 1958: Some hemispheric spectral statistics. *J. Meteor.*, **15**, 259–263.

Shapiro, R., and F. Ward, 1960: The time space-spectrum of the geostrophic meridional kinetic energy. *J. Meteor.*, **17**, 621–626.

Van der Hoven, I., 1957: Power spectrum of horizontal wind speed in the frequency range from 0.0007 to 900 cycles per hour. *J. Meteor.*, **14**, 160–164.

Van Mieghem, J., 1961: Zonal harmonic analysis of the Northern Hemisphere geostrophic wind field. (I.A.M.A.P. Presidential Address, Helsinki, 27 July 1960) I.U.G.G. Monogr. No. 8, Paris, 57 pp.

Wendell, Larry L., 1969: A study of the large-scale atmospheric turbulent kinetic energy in wavenumber-frequency space. *Tellus* (in press).